

## Dissociative recombination without a curve crossing

Steven L. Guberman

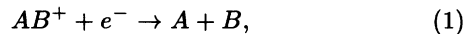
*Institute for Scientific Research, 33 Bedford Street, Lexington, Massachusetts 02173*

(Received 13 December 1993)

*Ab initio* calculations show that a curve crossing is not always needed for a high dissociative-recombination cross section. For  $\text{HeH}^+$ , in which no neutral states cross the ion potential curve, dissociative recombination is driven by the nuclear kinetic-energy operator on adiabatic potential curves. The kinetic-energy derivative operator allows for capture into repulsive curves that are outside of the classical turning points for the nuclear motion. The dominant dissociative route is the  $C^2\Sigma^+$  state leading to  $\text{H}(n=2)$  atoms. An analogous mechanism is proposed for the dissociative recombination of  $\text{H}_3^+$ .

PACS number(s): 34.80.Kw

A central feature of the dissociative-recombination (DR) mechanism [1] is that, in order for the cross section to be high, it is necessary that a repulsive potential curve controlling the motion of the products in (1),



cross the ion between the classical turning points of the recombining  $AB^+$  vibrational level. It is assumed in this mechanism that the dissociative curve is diabatic, i.e., it crosses other states of the same symmetry in order to reach the ion. However, recent experiments indicate that in both  $\text{HeH}^+$  and  $\text{H}_3^+$ , the DR rate at room temperature is greater than  $1.0 \times 10^{-9} \text{ cm}^3/\text{sec}$ , even though there appear to be no favorable crossings of the ion potential curve by a neutral dissociative curve. The presumed lack of an appropriate dissociative route in  $\text{HeH}$  has influenced the interpretation of the experimentally derived DR rates. A merged-beam experiment [2] on  $^4\text{HeH}$  gave a rough estimate of the rate to be  $10^{-8} \text{ cm}^3/\text{sec}$  at 300 K. A more recent merged-beam experiment [3] reports higher cross sections than those reported in Ref. [2]. Aware of the lack of a crossing of dissociative and ion potential curves, it was proposed that the high rate must be due to an excited  $a^3\Sigma^+$  ion state in the beam [3], and possibly to indirect recombination [4] in which a highly excited Rydberg state is populated prior to dissociation [2]. Relative cross sections for the recombination of  $^4\text{HeH}^+$  in the TARN II (Tokyo) storage ring have been reported [5]. Recent results indicate that the recombination is primarily to  $\text{H}(n=2)$  atoms [6]. The CRYRING (Stockholm) storage ring [7] has been used to study  $^3\text{HeH}^+$  recombination, and averaged cross sections have been reported. A preliminary report of a theoretical study of  $^4\text{HeH}^+$  DR using the  $R$  matrix approach has also appeared [8].

In the next section, we describe the calculation of the electronic wave functions. This is followed by a description of the derivative coupling which drives the recombination. An analysis of the coupling terms shows that the  $C$  state is the dominant dissociative route. Lastly, the calculated cross sections and rates for  $^3\text{HeH}$  are discussed and the important role of indirect recombination is demonstrated. These calculations use adiabatic potential curves and derivative couplings to drive DR.

## WAVE FUNCTIONS

The potential curves for  $\text{HeH}$  and  $\text{HeH}^+$  were calculated with contracted triple- $\zeta$  Gaussian basis sets [9] with a single  $4f$  primitive centered on each atom. The H basis set also included three additional diffuse  $s$  and four additional diffuse  $p$  basis functions for describing the lowest four  $^2\Sigma^+$  Rydberg states. The configuration-interaction (CI) wave functions were generated by taking all single and double excitations from a multiterm reference set. For the ground state at  $R = 1.0a_0$  and  $2.0a_0$  the calculated energies are only 0.0001 hartrees from the full CI energy. The potential curves are shown in Fig. 1. For the  $A^2\Sigma^+$  state, the calculated  $R_e$  agrees with the experimental  $^4\text{HeH}$  value [10] to four decimal places, and the  $\omega_e$  is  $18 \text{ cm}^{-1}$  smaller than the experimental value [10].

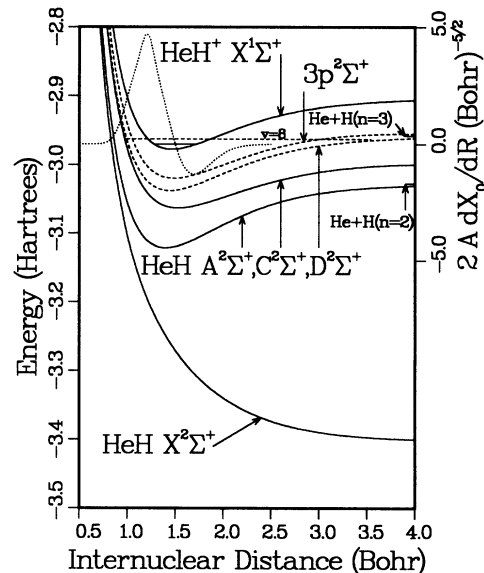


FIG. 1. The calculated  $\text{HeH}$  dissociative potential-energy curves (solid lines), the  $n=3$  Rydberg states (dashed lines), and the  $\text{HeH}^+$  ground state (solid line) with the  $v=0$  level are shown. The  $v=8$  resonance level of the  $D^2\Sigma^+$  state is shown as the dashed line. The dotted line shows the product,  $2A(R)d\chi_0/dR$ , with its ordinate axis on the right.

For  $C^2\Sigma^+$ , the calculated  $R_e$  is  $0.0035a_0$  smaller and the  $\omega_e$  is  $18\text{ cm}^{-1}$  larger than the experimentally derived values [10]. In addition to the HeH ground state, the  $A$  and  $C$  Rydberg states (shown as solid lines in Fig. 1) are also dissociative channels since the asymptote for these  $^3\text{HeH}$  states is  $1.56\text{ eV}$  below the  $v = 0$  level of the ion. Those states which go to the  $\text{H}(n = 3) + \text{He}$  asymptote (shown as dashed lines in Fig. 1) are  $0.33\text{ eV}$  above the  $v = 0$  level.

### KINETIC-ENERGY COUPLING

The direct DR cross section along one dissociative state from ion vibrational level  $v$ , i.e., without any Rydberg resonances, is given by [11]

$$\sigma_v = \left( \frac{\pi r}{2k_e^2} \right) \frac{4\xi_v}{\left( 1 + \sum_{v'} \xi_{v'} \right)^2}, \quad (2)$$

where  $k_e$  is the wave number of the incident electron,  $r$  is the ratio of the statistical weights of the neutral and ion states,  $v'$  is an index running over the open ion vibrational levels, and the  $\xi_v$  are given by

$$\xi_v = (\pi^2 \rho) [\langle \psi_d \chi_d | \mathcal{O} | \psi_v \chi_v \rangle]^2, \quad (3)$$

where  $d$  and  $v$  label dissociative and ion wave functions, respectively.  $\psi$  is the many-electron wave function ( $\psi_v$  includes the free-electron orbital),  $\chi$  is the corresponding vibrational wave function, and  $\mathcal{O}$  is the operator that connects the dissociative and ion plus free-electron states. In the integration over the electronic coordinates in (3), a Rydberg wave function is substituted for  $\psi_v$  and a density of states  $\rho$  is inserted in order to convert the matrix element to that appropriate for the electron-ion continuum. The density of states is calculated from the energy of the Rydberg state. In prior calculations of DR cross sections [12],  $\mathcal{O}$  has been the electronic Hamiltonian operator which connects the diabatic dissociative and Rydberg states. The diabatic valence states were defined by omitting Rydberg character. This procedure cannot be used for the dissociative HeH Rydberg states. As a result, adiabatic states are used. (Note that diabatic states could be defined and used here, but this approach would require that the adiabatic states and couplings be calculated first and transformed to diabatic states and couplings. The usage of diabatic states here is inconvenient.) For these states the electronic Hamiltonian matrix element connecting different states vanishes and  $\mathcal{O}$  is the nuclear kinetic-energy operator  $T_N$ ,

$$T_N = -\frac{\hbar^2}{2\mu} \frac{1}{R^2} \frac{\partial}{\partial R} R^2 \frac{\partial}{\partial R}, \quad (4)$$

where  $R$  is the internuclear distance,  $\hbar$  is Planck's constant, and  $\mu$  is the reduced mass. If  $\psi_d$  and  $\psi_v$  are orthogonal, after some manipulation we get for the interaction matrix element,

$$\begin{aligned} \langle \psi_d \chi_d | T_N | \psi_v \chi_v \rangle \\ = -\frac{\hbar^2}{2\mu} \left\langle \chi_d \left| B(R) + 2A(R) \frac{\partial}{\partial R} \right| \chi_v \right\rangle, \end{aligned} \quad (5)$$

where

$$B(R) = \left\langle \psi_d \left| \frac{\partial^2}{\partial R^2} \right| \psi_v \right\rangle \quad \text{and} \quad A(R) = \left\langle \psi_d \left| \frac{\partial}{\partial R} \right| \psi_v \right\rangle. \quad (6)$$

$A(R)$  and  $B(R)$  have been taken and derived respectively from the matrix elements in Ref. [13]. The important point here is that the values of  $A(R)$  and  $B(R)$  are of comparable magnitude, but the second term on the right-hand side of Eq. (5) involves the derivative of the vibrational wave function and is large in the region of interest for DR. At the energy of the  $v = 0$  ion level and at the turning points of the calculated continuum vibrational levels in the  $X$ ,  $A$ , and  $C$  states of  $^3\text{HeH}$ , the ratio of the derivative of the  $v = 0$  wave function to the  $v = 0$  wave function is  $24a_0^{-1}$ ,  $22a_0^{-1}$ , and  $16a_0^{-1}$  and the value of the derivative is  $0.0581a_0^{-3.2}$ ,  $0.1156a_0^{-3/2}$  and  $0.7559a_0^{-3/2}$ , respectively. For the DR cross section to be large,  $A(R)$  must not be negligible where the derivative of the vibrational wave function is large.  $A(R)$  is non-negligible in regions where there is an exchange of character between states. This is the case in HeH, where there is an avoided crossing between the  $X$  and  $A$  states and between the  $C$  and  $D$  states near  $(0.7-0.8)a_0$  [14]. The dotted line of Fig. 1 shows a plot of  $2A(R)d\chi_0/dR$  [from the second term of Eq. (6)], where  $A(R)$  is that between the  $C$  and  $D$  states. For internuclear distances smaller than the inner turning point of the ion  $v = 0$  level, this product is the largest in these calculations and has considerable amplitude near the turning point of the repulsive neutral  $C$  state. The second most important product is that for which the  $A$  matrix element is between the  $C$  and  $3p$  states. The derivative operator enlarges the range of  $R$  over which DR can occur allowing for high DR rates in the absence of a curve crossing. From the shape of the product, we would expect its overlap to be greatest with the continuum vibrational wave function for the  $C$  state and much smaller with that for the  $X$  and  $A$  states. These predictions are supported by the results of the full cross-section calculations discussed below and by the TARN II storage ring results [6] (see below) and are contrary to the  $R$  matrix results [8] which found that the  $X$  state has the largest DR cross section.

### CROSS SECTIONS AND RATES

The cross sections were calculated using the multichannel quantum-defect-theory (MQDT) approach described previously [11,15], with some revisions to account for the three dissociative routes and the two-electron angular momenta used here. Nine vibrational levels in the ion and Rydberg states were included. The only nonzero  $K$  matrix elements included are those connecting the dis-

sociative channels to the ion or Rydberg levels. The interaction between the dissociative states due to the nuclear kinetic-energy operator was neglected. This approximation is justified because the total cross section is almost entirely due to the  $C$  state and the  $C$  state has only a small interaction with the  $X$  and  $A$  states [13,14]. The interaction between the ion or Rydberg levels is accounted for in the frame transformation [11,15]. Details on the calculation of the  $K$  matrix and the electron angular momenta mixing matrix [16] will be published separately. The quantum defects were taken from the energies calculated for the  $D$  and  $3p^2\Sigma^+$  states. The Rydberg series associated with each of these states are denoted " $l$ "=0 and " $l$ "=1, respectively. Figure 2 shows the total cross section for  ${}^3\text{HeH}$  over electron energies ranging from 0.001 to 0.33 eV. The dashed line is for direct DR only [from Eq. (2)] and the solid line is for total DR including the Rydberg resonance levels. The total cross section at 0.001 eV is  $1.3 \times 10^{-13}$  cm<sup>2</sup> and is almost entirely due to the  $C$  state. Calculated cross sections along the  $X$  and  $A$  states are three to four orders of magnitude smaller than  $C$  state cross sections. Therefore the dissociation products will nearly always include an excited  $n = 2$  H atom, in agreement with the recent TARN II storage ring results [6]. At 0.001 eV, the indirect DR mechanism due to the Rydberg resonances plays an important role where we see that the full cross section is about two orders of magnitude larger than the direct cross section. The importance of indirect recombination is in agreement with the earlier speculation of Yousif and Mitchell [2]. Labeling the resonances as  $(n, v, "l")$ , this effect is due to the (4,2,1) resonance which causes the peak near 0.002 eV. Interference between the (6,1,1) and

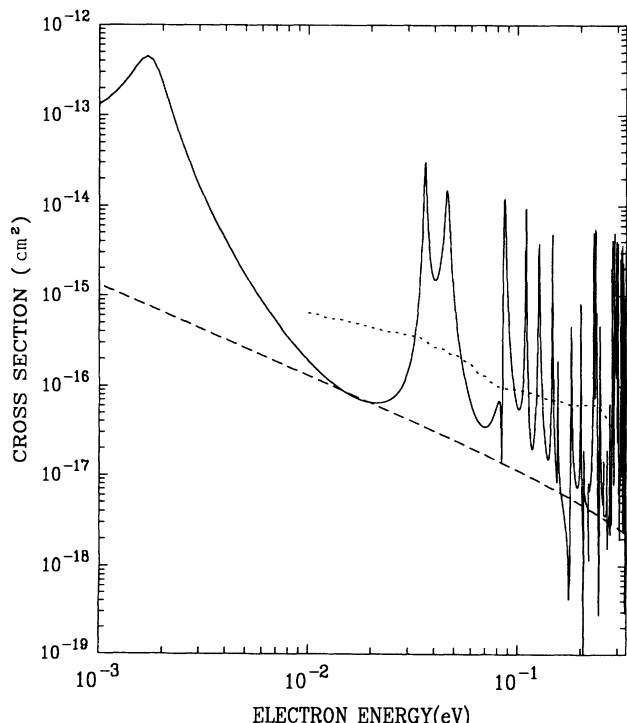


FIG. 2. The calculated direct DR cross section (dashed line), the full DR cross section (solid line), and the result of Larsson *et al.* [7] (dotted line) for  ${}^3\text{HeH}$ .

(3,4,1) resonances leads to the double peak near 0.04 eV. The narrow peak near 0.8 eV is due to (7,1,0). The " $l$ "=1 resonances dominate the low energy recombination. The  $v = 8$  resonance level shown in Fig. 1 is the source of the peak at 0.16 eV. The averaged cross sections from the CRYRING experiment ( $\langle\sigma v\rangle/v$ , where  $v$  is the electron velocity) are shown as the dotted line [7]. These cross sections do not show resonance structure because they take into account the experimental electron velocity distribution characterized by a transverse electron temperature of 0.1 eV. The agreement with the calculated results is excellent. Recent unpublished experimental results of Mowat *et al.* [17] at a transverse electron temperature of 0.01 eV clearly show the prominent resonances identified above. These calculations show that recombination from the  $\text{HeH}^+$  ground state can indeed yield a non-negligible cross section. Agreement with the structure seen in the most recent CRYRING results rules out the possible role of a metastable triplet ion state suggested in Ref. [3]. The rate for  ${}^3\text{HeH}$  DR for electron temperatures ( $T_e$ ) between 200 and 400 K calculated from a Maxwellian average over the cross section is  $2.6 \times 10^{-8} \times (T_e/300)^{-4.7}$  cm<sup>3</sup>/sec. In additional calculations, we have found that the calculated cross sections are sensitive to the isotopomer under study. Comparison to the merged-beam results will be reported separately.

In  $\text{H}_3^+$ , the energetics are such that the Rydberg states cannot provide routes for DR of the lowest vibrational level at low electron energies. However, in  $\text{HeH}$ , the  $X$ - $A$  derivative coupling is large and similar to the  $C$ - $D$  coupling. If we substitute the  $X$ - $A$  coupling for the  $C$ - $D$  coupling, the  $2A(d\chi_0/dR)$  product would be quite similar to that shown in Fig. 1. We can therefore envision  $\text{HeH}$  in its ground state, at an internuclear separation of about  $1.0a_0$ , with the He split perpendicular to the  $\text{HeH}$  axis into two H atoms at very small separation, giving a  ${}^2A_1$  state. The coupling between this  ${}^2A_1$  state and the lowest  ${}^2A_1$  Rydberg state should resemble the  $\text{HeH}$   $X$ - $A$  coupling.

## SUMMARY

The calculations presented here show that large cross sections and rates can be found in  ${}^3\text{HeH}$  where there is no crossing of a dissociative potential curve with the ion curve. Consideration of the overlap between the continuum nuclear wave function in the dissociative state and the product of the derivative of the ion wave function with the  $A$  matrix element shows that the  $C$  state is the dominant dissociative channel, and this is confirmed with the MQDT calculations. Indirect recombination [4] through the Rydberg states plays a prominent role.

## ACKNOWLEDGMENTS

This work is supported by NASA Grants NAGW 2832 and 1404 and by NSF Grant No. ATM9122739. The computations were done at the National Center for Atmospheric Research and at the Pittsburgh Supercomputer Center, which are both supported by NSF. I am grateful to Mats Larsson, Annick Suzor-Weiner, and Wim van der Zande for valuable discussions. I thank I. D. Petsalakis for helpful correspondence and T. Tanabe for providing his results prior to publication.

- [1] See, e.g., J. N. Bardsley and M. A. Biondi, *Adv. At. Mol. Phys.* **6**, 1 (1970).
- [2] F. B. Yousif and J. B. A. Mitchell, *Phys. Rev. A* **40**, 4318 (1989).
- [3] F. B. Yousif, J. B. A. Mitchell, A. Canosa, and M. I. Chibisov, in *Book of Abstracts of the Eighteenth International Conference on the Physics of Electronic and Atomic Collisions, Aarhus, 1993* (Aarhus University, Aarhus, 1993), p. 662.
- [4] J. N. Bardsley, *J. Phys. B* **1**, 365 (1968).
- [5] T. Tanabe *et al.*, *Phys. Rev. Lett.* **70**, 422 (1993).
- [6] T. Tanabe *et al.*, *Phys. Rev. A* **49**, R1531 (1994).
- [7] M. Larsson *et al.*, in *The Physics of Electronic and Atomic Collisions, XVIII International Conference, Aarhus, 1993*, edited by T. Andersen, B. Fastrup, F. Folkmann, H. Knudsen, and N. Andersen, AIP Conf. Proc. No. 295 (AIP, New York, 1993), p. 803.
- [8] B. K. Sarpal, J. Tennyson, and L. A. Morgan, in *Book of Abstracts of the Eighteenth Conference on the Physics of Electronic and Atomic Collisions, Aarhus, 1993* (Ref. [3]), p. 386; B. K. Sarpal, J. Tennyson, and L. A. Morgan (unpublished).
- [9] P.-O. Widmark, P.-A. Malmqvist, and B. O. Roos, *Theor. Chim. Acta* **77**, 291 (1990).
- [10] W. Ketterle, A. Dodhy, and H. Walther, *J. Chem. Phys.* **89**, 3442 (1988).
- [11] A. Giusti, *J. Phys. B* **13**, 3867 (1980).
- [12] S. L. Guberman, in *Dissociative Recombination: Theory, Experiment, and Applications*, edited by J. B. A. Mitchell and S. L. Guberman (World Scientific, Teaneck, NJ, 1989), p. 45.
- [13] I. D. Petsalakis, G. Theodorakopoulos, C. A. Nicolaides, and R. J. Buenker, *J. Phys. B* **20**, 5959 (1987).
- [14] C. Kubach, V. Sidis, D. Fussen, and W. J. van Der Zande, *Chem. Phys* **117**, 439 (1987); M. C. van Hemert and S. D. Peyerimhoff, *J. Chem. Phys.* **94**, 4369 (1991).
- [15] S. L. Guberman and A. Giusti-Suzor, *J. Chem. Phys.* **95**, 2602 (1991).
- [16] H. Takagi, N. Kosugi, and M. Le Dourneuf, *J. Phys. B* **24**, 711 (1991).
- [17] J. R. Mowat *et al.* (unpublished).